Supplementary Information

Alkylammonium passivation for 2D tin halide perovskite field-effect transistors

Hakjun Kim,[a,‡] Cheong Beom Lee,[b,c,‡] Bum ho Jeong,[a] Jongmin Lee,[a] Jia Choi,[a] Kyeounghak Kim,[c,*] Hui joon Park[a,d,*]

[a]Department of Organic and Nano Engineering & Human-Tech Convergence Program, Hanyang University, Seoul 04763, Republic of Korea

[b]Department of Chemistry, Hanyang University, Seoul 04763, Republic of Korea

[c]Department of Chemical Engineering, Hanyang University, Seoul 04763, Republic of Korea

[d]Department of Semiconductor Engineering, Hanyang University, Seoul 04763, Republic of Korea

[‡]These authors contribute equally to this work

[*]Corresponding authors

E-mail: huijoon@hanyang.ac.kr, chemekim@hanyang.ac.kr

Keywords: Sn halide perovskite, transistor, alkylammonium, defect-passivation

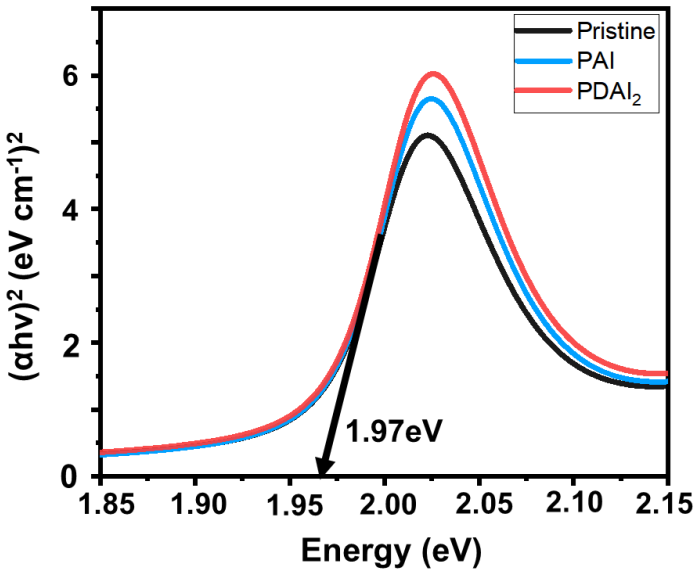

Figure S1. Tauc plots of $(PEA)_2SnI_4$ thin films with and without additives (PAI and $PDAI_2$).

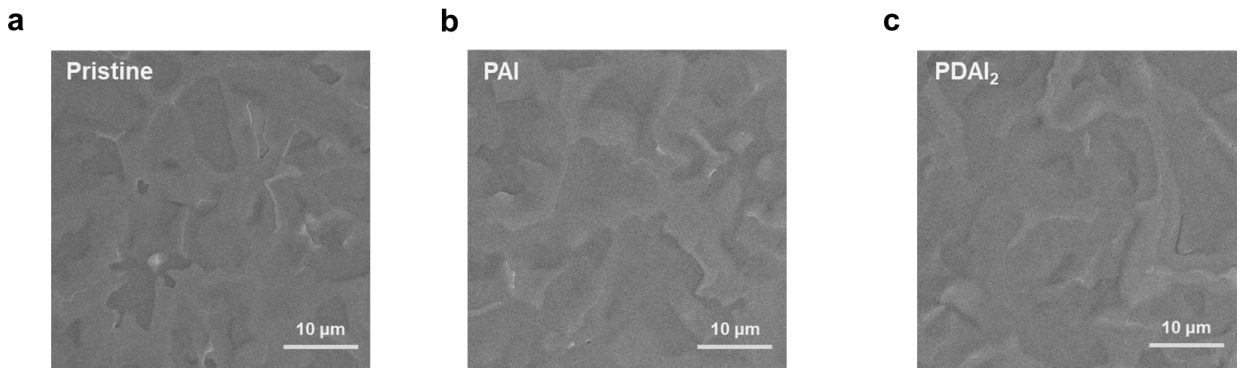

Figure S2. SEM images of (a) pristine $(PEA)_2SnI_4$ films, (b) $(PEA)_2SnI_4$ film with PAI, and (c) $(PEA)_2SnI_4$ film with $PDAI_2$ (scale bar: 10 μm).

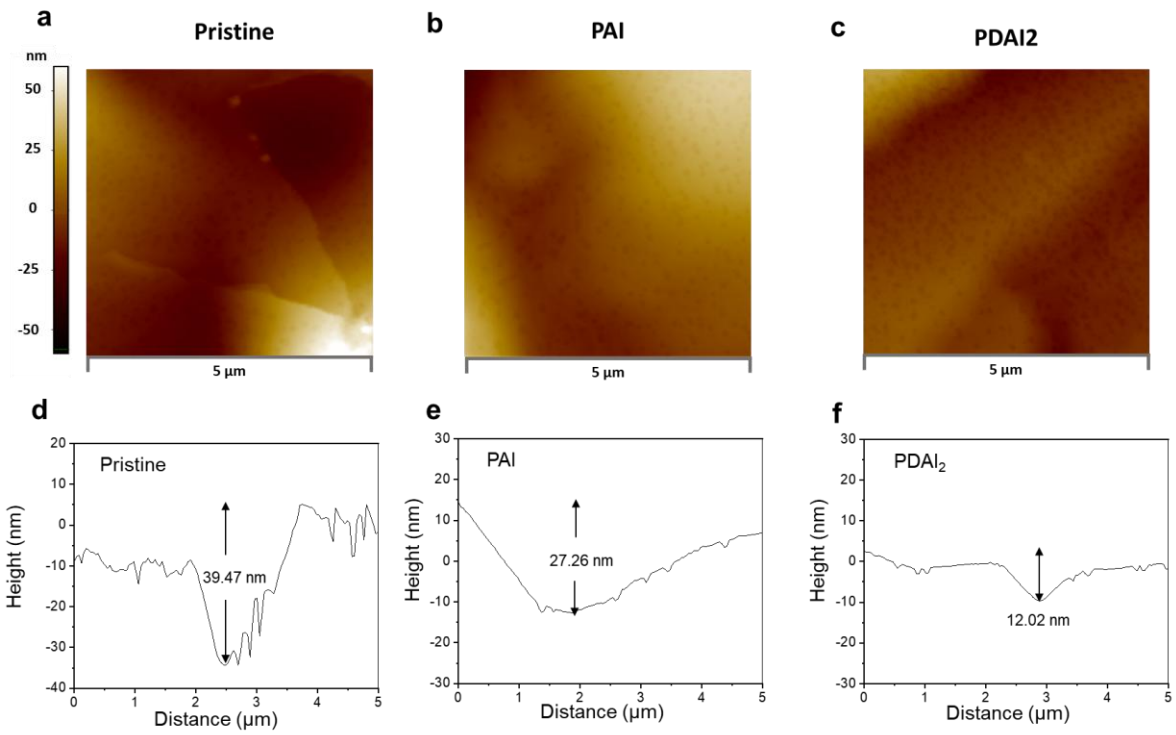

Figure S3. Non-contact mode atomic force microscope (AFM) images of (a) pristine $(PEA)_2SnI_4$ films, (b) $(PEA)_2SnI_4$ film with PAI, and (c) $(PEA)_2SnI_4$ film with $PDAI_2$, along with their corresponding height profiles in (d), (e), (f), respectively.

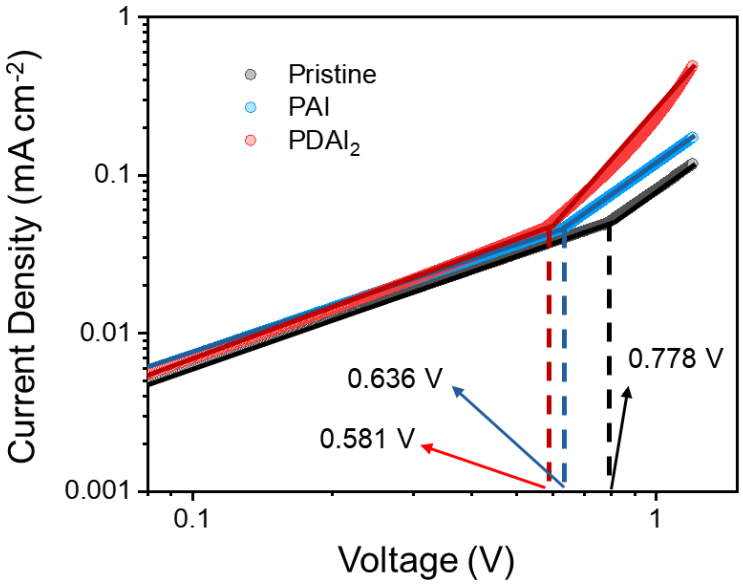

Figure S4. SCLC measurements of hole-only devices based on $(PEA)_2SnI_4$ thin films with and without additives (PAI and $PDAI_2$).

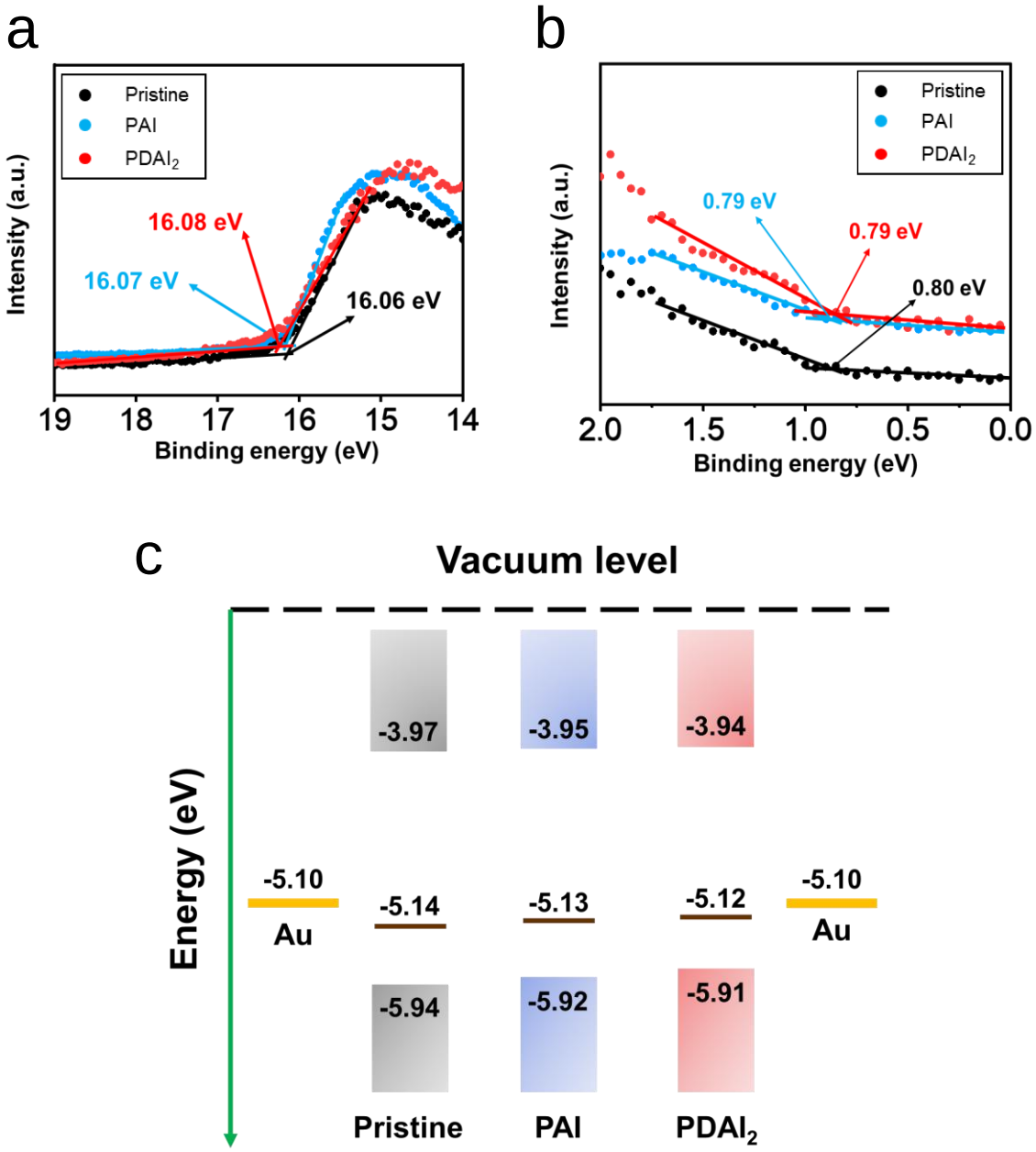

Figure S5. UV photoelectron spectroscopy (UPS) analysis. (a) Secondary electron cut-off region of $(PEA)_2SnI_4$ film with and without additives (PAI and $PDAI_2$). (b) Onset region of $(PEA)_2SnI_4$ film with and without additives (PAI and $PDAI_2$). (c) Energy band structures of $(PEA)_2SnI_4$ film with and without additives (PAI and $PDAI_2$).

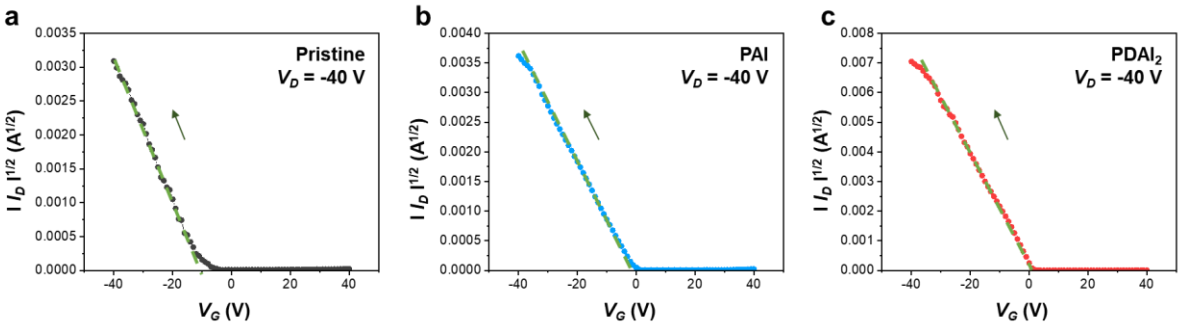

Figure S6. Transfer characteristics ($V_G - \sqrt{|I_D|}$) of $(PEA)_2SnI_4$ FETs with and without additives (a) Pristine (b) PAI added (c) $PDAI_2$ added. The green dashed lines represent the slope used to calculate the claimed mobility (μ_{claimed}) under the forward scan.

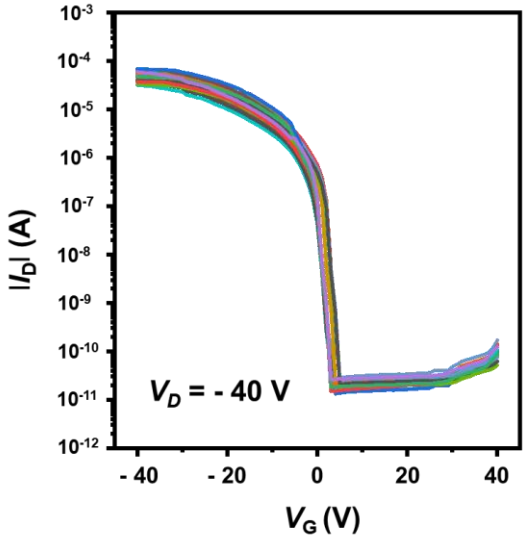

Figure S7. Transfer curves of 30 different $(PEA)_2SnI_4$ FET devices with $PDAI_2$ (V_D = -40 V) (forward scan).

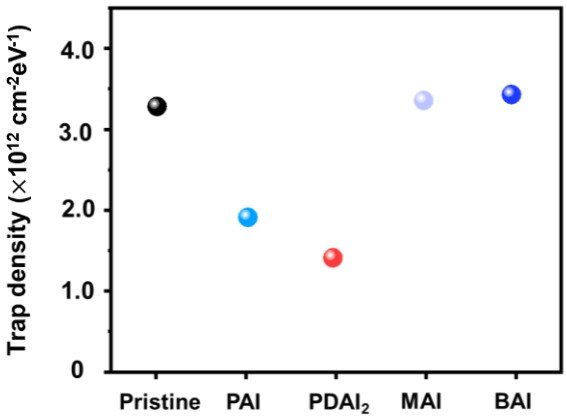

Figure S8. Maximum trap density within $(PEA)_2SnI_4$ FET devices with and without additives (PAI, $PDAI_2$, MAI, and BAI).

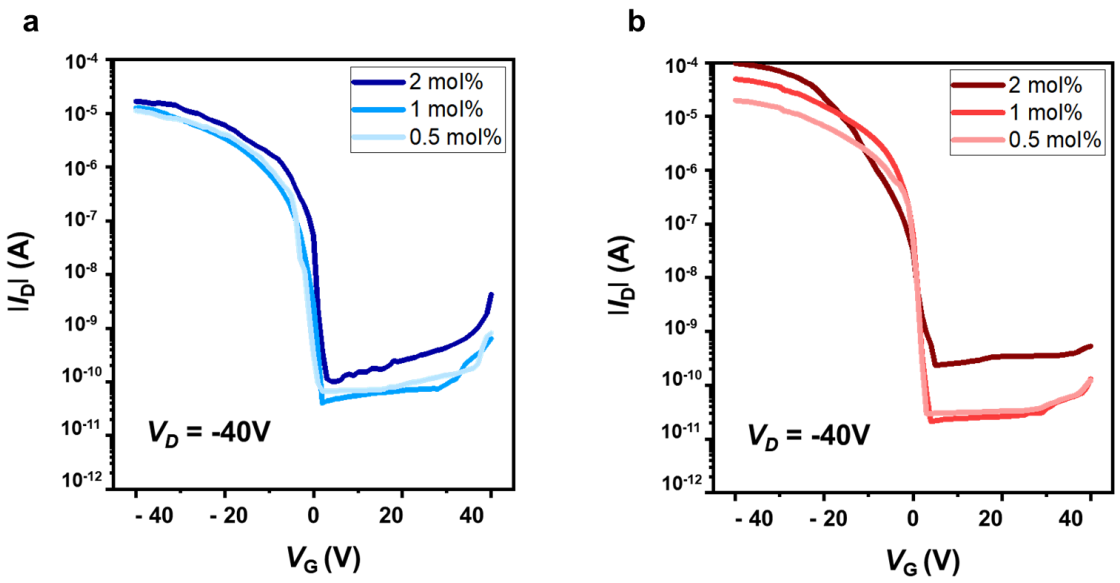

Figure S9. Transfer characteristics of $(PEA)_2SnI_4$ FET devices as a function of additive concentration. (a) PAI. (b) $PDAI_2$.

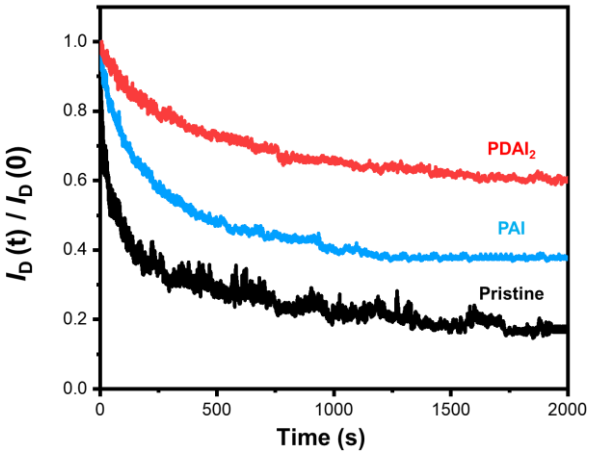

Figure S10. Bias-stress stability of $(PEA)_2SnI_4$ FETs with and without additives (PAI and $PDAI_2$) for over 2000 s under constant bias condition (V_G = -40 V and V_D = -40 V).

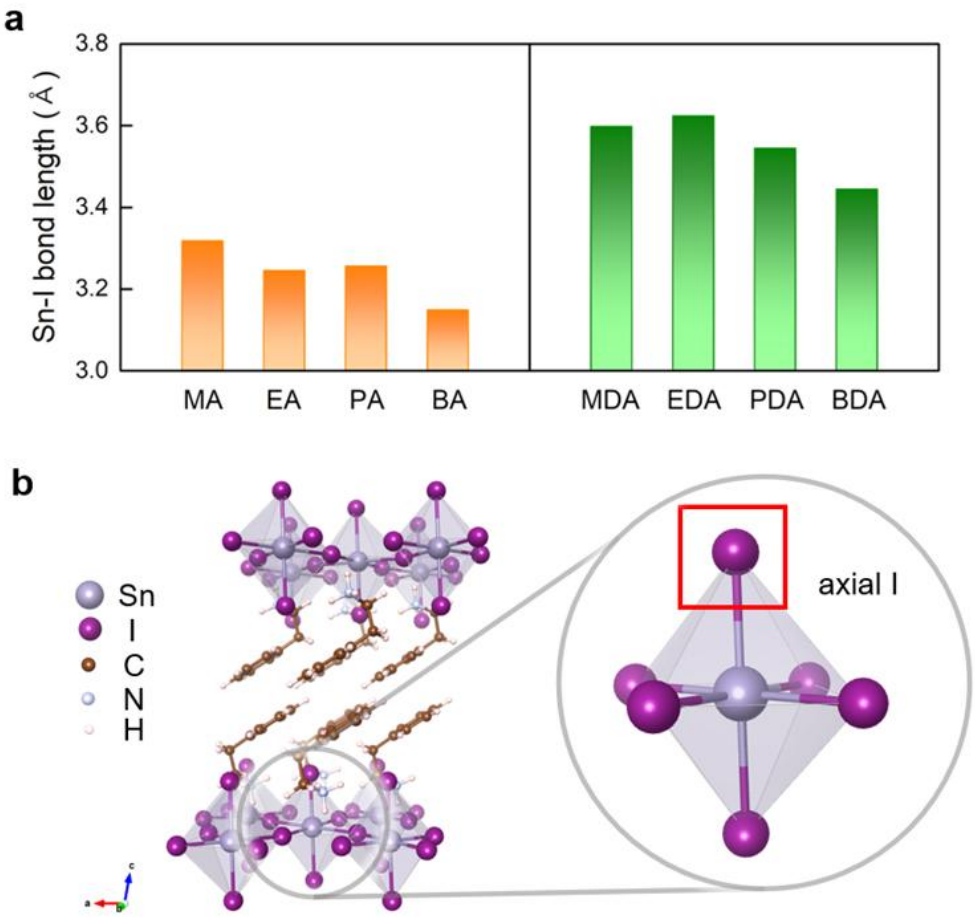

Figure S11. (a) Bond lengths of Sn–axial I in 2D perovskites with the addition of MA, EA, PA, BA, MDA, EDA, PDA, and BDA cations. (b) Schematic figure of axial I in the inorganic framework. The axial I is represented by red square.

Note 1. Calculations of mobility values of $(PEA)_2SnI_4$ FETs

In the saturation region of a FET device, threshold voltage (V_{th}) and field-effect mobility (μ_{FE}) can be calculated using the following equations.[1]

$$I_{\mathrm{D,sat}} = \frac{\mu_{\mathrm{FE,sat}} W C_{\mathrm{i}}}{2L}(V_G - V_{th})^2, |V_{\mathrm{G}} - V_{\mathrm{th}}| < |V_{DS}|$$

$$\mu_{FE,\mathrm{sat}} = \frac{2L}{WC_{\mathrm{i}}}\left(\frac{\partial\sqrt{|I_{\mathrm{D}}|}}{\partial V_{\mathrm{G}}}\right)^2$$

where V_{G} and I_{D} are the source-to-gate voltage and the source-to-drain currents, respectively. And L, W, C_{i} represent the channel length, width, and unit capacitance of the oxide dielectric layer, respectively.

Due to nonidealities such as contact effects, charge trapping, and ion migration, careful evaluation is required for accurate mobility extraction. To minimize potential errors in mobility assessment, we calculated the reliability factor (r_{sat}), along with the effective mobility (μ_{eff}).[2]

$$r_{\mathrm{sat}} = \left(\frac{\sqrt{|I_{\mathrm{D}}|^{\mathrm{max}}} - \sqrt{|I_{\mathrm{D}}^{\mathrm{o}}|}}{|V_{\mathrm{G}}|^{\mathrm{max}}}\right)^2 / \left(\frac{\partial\sqrt{|I_{\mathrm{D}}|}}{\partial V_{\mathrm{G}}}\right)^2_{\mathrm{claimed}}$$

$$\mu_{\mathrm{eff}} = r_{\mathrm{sat}} \times \mu_{\mathrm{claimed}}$$

where $|I_{\mathrm{D}}|^{\mathrm{max}}$ and $|I_{\mathrm{D}}^{\mathrm{o}}|$ are the maximum source-to-drain current at the maximum gate voltage ($|V_{\mathrm{G}}|^{\mathrm{max}}$ = -40 V) and at $V_{\mathrm{G}} = 0\,V$. The effective mobility values and the reliability factor for $(PEA)_2SnI_4$ FETs, with and without additives (PAI and $PDAI_2$), are summarized in Table S1.

Table S1. Evaluation of field-effect mobility values for $(PEA)_2SnI_4$ FETs with and without additives (PAI and $PDAI_2$). Data are obtained from the highest-performing device under each condition.

		Pristine	PAI	$PDAI_2$
$\mu_{claimed}$ ($cm^2 V^{-1} s^{-1}$)	**Forward**	0.62	1.37	2.60
	Reverse	0.86	2.46	3.31
r_{sat} (%)	**Forward**	12.1	54.6	76.1
	Reverse	13.8	38.5	45.8
$\mu_{effective}$ ($cm^2 V^{-1} s^{-1}$)	**Forward**	0.08	0.75	1.98
	Reverse	0.12	0.95	1.52

References in Supplementary Information

1. S. M. Sze and K. K. Ng, *Physics of Semiconductor Devices*, 3rd edn, John Wiley & Sons, 2007.

2. H. H. Choi, K. Cho, C. D. Frisbie, H. Sirringhaus and V. Podzorov, *Nat. Mater.*, 2018, **17**, 2–7, DOI: 10.1038/nmat5035.